Biochimica et Biophysica Acta 1813 (2011) 1740–1748

Contents lists available at ScienceDirect

Biochimica et Biophysica Acta

journal homepage: www.elsevier.com/locate/bbamcr

Mitochondria adjust Ca^{2+} signaling regime to a pattern of stimulation in salivary acinar cells

Olga Kopach [a,1], Ilya Kruglikov [b,2], Tatyana Pivneva [a,3], Nana Voitenko [a,4], Alexei Verkhratsky [c,5], Nataliya Fedirko [a,*,6]

[a] Department of General Physiology of Nervous System, Bogomoletz Institute of Physiology, Kiev 01024, Ukraine
[b] Department of Physiology and Neuroscience, New York University School of Medicine, NY 10016, USA
[c] Faculty of Life Sciences, The University of Manchester, United Kingdom

ARTICLE INFO

Article history:
Received 9 December 2010
Received in revised form 27 February 2011
Accepted 23 March 2011
Available online 30 March 2011

Keywords:
Store-operated calcium entry
Mitochondria
Endoplasmic reticulum
Ca^{2+} microdomains
Submandibular acinar cells

ABSTRACT

The salivary acinar cells have unique Ca^{2+} signaling machinery that ensures an extensive secretion. The agonist-induced secretion is governed by Ca^{2+} signals originated from the endoplasmic reticulum (ER) followed by a store-operated Ca^{2+} entry (SOCE). During tasting and chewing food a frequency of parasympathetic stimulation increases up to ten fold, entailing cells to adapt its Ca^{2+} machinery to promote ER refilling and ensure sustained SOCE by yet unknown mechanism. By employing a combination of fluorescent Ca^{2+} imaging in the cytoplasm and inside cellular organelles (ER and mitochondria) we described the role of mitochondria in adjustment of Ca^{2+} signaling regime and ER refilling according to a pattern of agonist stimulation. Under the sustained stimulation, SOCE is increased proportionally to the degree of ER depletion. Cell adapts its Ca^{2+} handling system directing more Ca^{2+} into mitochondria via microdomains of high $[Ca^{2+}]$ providing positive feedback on SOCE while intra-mitochondrial tunneling provides adequate ER refilling. In the absence of an agonist, the bulk of ER refilling occurs through Ca^{2+}-ATPase-mediated Ca^{2+} uptake within subplasmalemmal space. In conclusion, mitochondria play a key role in the maintenance of sustained SOCE and adequate ER refilling by regulating Ca^{2+} fluxes within the cell that may represent an intrinsic adaptation mechanism to ensure a long-lasting secretion.

1. Introduction

The submandibular salivary gland provides a major contribution to the secretion of fluid and electrolytes [1,2]. Salivary flow occurs in two distinct modes: resting secretion occurring at a low rate and evoked secretion stimulated by the tasting and chewing food when more intense and/or frequent stimuli increase salivation up to ten fold. Evoked secretion is activated by acetylcholine (ACh), secreted by parasympathetic nerves [1,2]. ACh-induced fluid secretion is mediated by a complex $[Ca^{2+}]_{cyt}$ signal that is required for a synchronized activation of apical Ca^{2+}-dependent Cl^- channels and basolateral K^+ channels driving water flow out of the gland [2]. Prolonged salivation, which occurs during the ingestion of a meal, is initiated by an $InsP_3$-mediated Ca^{2+} release from the endoplasmic reticulum (ER) but subsequently depends on the $[Ca^{2+}]_{cyt}$ increase that is maintained by store-operated Ca^{2+} entry (SOCE) [1–3]. The acinar cells are characterized by a specific structural and functional polarization and extremely developed ER, which substantially exceeded the ER in other cell types [2,4]. Under intense stimulation, the decrease in the ER (or intraluminal) level of Ca^{2+} ($[Ca^{2+}]_{ER}$) due to $InsP_3$ receptors activity may alter ER protein synthesis and processing, triggering ER stress response [5]. Therefore the acinar cell needs to undergo an adaptational change in Ca^{2+} signaling to promote the ER refilling and sustained SOCE necessary for a prolonged salivation.

Molecular mechanisms responsible for SOCE in acinar cells are not completely understood, although trans-membrane transient receptor potential channel 1 (TRPC1) is reported to be a core component of the store-operated channel (SOC) [6,7]. Recently, it was shown that two other proteins STIM1 and Orai1 can reconstitute store-activated trans-

Abbreviations: ACh, acetylcholine; $[Ca^{2+}]_{cyt}$, cytosolic Ca^{2+} concentration; ER, endoplasmic reticulum; PM, plasma membrane; $InsP_3$, inositol 1,4,5-trisphosphate; $[Ca^{2+}]_{ER}$, ER Ca^{2+} concentration; $[Ca^{2+}]_{mit}$, mitochondrial Ca^{2+} concentration; SOC, store-operated channel; SOCE, store-operated Ca^{2+} entry; PMCA, Ca^{2+} ATPase of PM; SERCA, Ca^{2+} ATPase of the ER; NCX, mitochondrial Na^+/Ca^{2+} exchanger; TRPC1, transient receptor potential channel 1; TG, thapsigargin; EM, electron microscopy; FCCP, p-trifluoromethoxy carbonyl cyanide phenyl hydrazone; CGP37157, 7-Chloro-5-(2-chlorophenyl)-1,5-dihydro-4,1-benzothiaze pin-2(3H)-one

* Corresponding author at: Department of General Physiology of Nervous System, Bogomoletz Institute of Physiology, 4 Bogomoletz Str., Kiev 01024, Ukraine. Tel.: +38 044 2562428; fax: +38 044 256 2053.
E-mail address: n_fedirko@biph.kiev.ua (N. Fedirko).

[1] Olga Kopach: acquisition of data, data analysis and interpretation; statistical analysis.
[2] Ilya Kruglikov: data analysis and interpretation; material support.
[3] Tatyana Pivneva: acquisition of electron microscopy data.
[4] Nana Voitenko: technical, material support.
[5] Alexei Verkhratsky: critical revision of the manuscript.

0167-4889/$ – see front matter.
doi:10.1016/j.bbamcr.2011.03.016

membrane currents in other cell types [8]. In salivary cells, all 3 proteins are required for the induction of SOCE in response to the ER depletion; they form TRPC1–STIM1–Orai1 ternary complex in the ER–PM lipid rafts domains [9–11]. The genetic deletion of even one protein of the complex results in a dramatic decrease of SOCE and Ca^{2+}-dependent K^+ currents [7]. Mutant TRPC1$^{-/-}$ animals demonstrate severe impairment of fluid secretion highlighting the importance of SOCE in the maintaining of physiological function of salivary cells [7].

Although Ca^{2+} entry is required for salivation, a cell needs to maintain the balance between Ca^{2+} influx and clearance resisting the risk of Ca^{2+} overload. Cytosolic Ca^{2+} clearance is accomplished by PMCA and SERCA as well as by Ca^{2+} uptake via Ca^{2+} uniporter of mitochondria [1,12]. Mitochondrial Ca^{2+} uptake is involved in the regulation of SOCE by preventing Ca^{2+}-dependent inactivation of SOCs [13,14]; in addition, mitochondrial respiration can control activation of SOCE [15]. Ca^{2+} taken up by mitochondria is subsequently released through the mitochondrial Na^+/Ca^{2+} exchanger (NCX) and may provide an additional source of Ca^{2+} for ER refilling. Hence, mitochondria are likely to be an adaptation system controlling interplay between SOCE and sustained ER refilling under prolonged stimulation.

In the present study, we aimed to define the mechanism of acinar cell adaptation under sustained agonist stimulation. We utilized a set of calcium imaging techniques to characterize the role of mitochondria in adjusting of Ca^{2+} signaling regime to a pattern of agonist stimulation.

2. Materials and methods

2.1. Isolation of submandibular acinar cells, extracellular solutions

Male 150–200 g Wistar rats were used in all experiments in accordance with protocols of the Animal Care and Use Committee at the Bogomoletz Institute. Acinar cells were isolated from the submandibular salivary gland using collagenase digestion as described previously [16,17]. The extracellular solution contained (in mM): NaCl 135, KCl 5, HEPES/NaOH 10, $MgCl_2$ 2, $CaCl_2$ 2, glucose 10, pH 7.35. For Ca^{2+}-free solution, $CaCl_2$ was omitted, $MgCl_2$ was increased to 4 mM and 1 mM EGTA was added.

2.2. Calcium imaging and electrophysiology

For measuring $[Ca^{2+}]_{cyt}$ cells were loaded with fura-2/AM (5 μM) as described previously [16]. Briefly, dye-loaded cells were alternately excited at 360 and 390 nm; emission was recorded at 510 ± 10 nm. Epifluorescent images were captured using the Olympus BX50WI fixed-stage microscope (New York/New Jersey Scientific, NJ, USA) fitted with a 60× (0.90 NA) water immersion objective and a high-sensitivity cooled CCD camera (Sensicam, PCO, Germany). The images were acquired in the fast mode using 2×2 binning with a temporal resolution of ~300 ms per frame The excitation light was delivered by a monochromator (Polychrom IV, TILL Photonics, Germany) at a cycle frequency of 6 Hz. Imaging Workbench 2.2 software (Axon Instruments/Molecular devices, Union City, CA) was used for controlling the monochromator and image acquisition.

For monitoring free Ca^{2+} concentration inside the ER ($[Ca^{2+}]_{ER}$) cells were loaded with a low-affinity Ca^{2+} dye mag-fura-2/AM (6 μM) as described elsewhere [17,18]. The cytosolic portion of mag-fura-2 was washed out in the whole-cell configuration [17]. Electrophysiological recordings were made using the Patch Clamp PC-505B amplifier (Warner Instruments, Hamden, USA) and digitized by a Digidata board 1320A (Molecular Devices), which was controlled by Clampex 8.2 software (Molecular Devices). Membrane potential was held at −40 mV. The intrapipette solution contained (in mM): K-gluconate 133, NaCl 5, $MgCl_2$ 0.5, HEPES/KOH 10, Mg-ATP 2, Na-GTP 0.5, pH to 7.2 and the final osmolarity 280–290 mOsm. To buffer free Ca^{2+} inside the pipette, intrapipette solution was supplemented either with 5 mM EGTA or with 5 mM BAPTA, as indicated in the text. $[Ca^{2+}]_{ER}$ was expressed as the changes in a ratio of mag-fura-2 fluorescence (F_{340}/F_{380}).

Mitochondrial $[Ca^{2+}]$ was measured with rhod-2/AM (5 μM) as described previously [17]. The cytosolic portion of the dye was washed out using patch-clamp approach. Rhod-2 was excited at 543 nm; emission was recorded at 576 nm. $[Ca^{2+}]_{mit}$ was expressed as the changes in rhod-2 fluorescence over the baseline ($\Delta F/F_0$). The baseline fluorescence (F_0) was defined as the cell fluorescence prior to stimulation and after the subtraction of background fluorescence.

2.3. Electron microscopy

Isolated clusters of acinar cells were fixed with 2% paraformaldehyde and 2% glutaraldehyde in 0.1 M phosphate buffer (PB, pH = 7.4) for 12 h at 4 °C; subsequently rinsed in cold PB and post-fixed in a solution containing 1% of osmium tetroxide, see also [12]. Cells were dehydrated in the increasing series of ethanol, pre-embedded with propylene oxide, and embedded in Epoxid resin (Plano, Wetzlar, Germany). Ultrathin sections (60–70 nm), after their post-staining with lead citrate and uranyl acetate, were examined with a JEM electron microscope (JEOL, Japan) at 80 kV.

2.4. Data analysis

All data are expressed as mean ± S.E.M. Statistical significance was calculated using paired and unpaired Student's *t*-test where appropriate; for multiple comparisons ANOVA analysis of variance was utilized. *p* Values<0.05 were considered as statistically significant. Each trace shown is representative of at least five independent experiments.

3. Results

3.1. The amplitude and kinetics of SOCE-mediated $[Ca^{2+}]_{cyt}$ transients directly correlate with a pattern of ER depletion

To visualize SOCE-mediated $[Ca^{2+}]_{cyt}$ transients, we depleted the ER in Ca^{2+}-free extracellular solution with either acetylcholine (ACh, 5 μM) or SERCA inhibitor thapsigargine (TG) or with both agents. Subsequently 2 mM Ca^{2+} was added to the extracellular solution producing Ca^{2+} influx (Fig. 1). In order to mimic conditions when cells are subjected to either single or several stimuli, we used two different protocols of ACh application: short (15 s, Fig. 1A) and prolonged (5 min, Fig. 1C, D). In the latter case Ca^{2+} entry was induced in the continuing presence of an agonist.

The magnitudes of the SOCE-mediated $[Ca^{2+}]_{cyt}$ transients strongly correlates with the degree of ER depletion (Fig. 2B, C). SOCE-induced $[Ca^{2+}]_{cyt}$ transients with the lowest amplitude were produced when the ER was depleted by a short ACh application (73 ± 7 nM, $n = 29$; Figs. 1A, 2A, C), while SOCE with the highest amplitude were produced when the ER was depleted by a prolong ACh application (332 ± 23% vs short ACh, $n = 18$, $p<0.001$; Figs. 1C, 2A, C). Depletion of the ER by TG or by prolong ACh application in the presence of TG caused significant increase of the mean amplitude of SOCE-induced $[Ca^{2+}]_{cyt}$ transients (by 151 ± 19%, $n = 10$, $p<0.01$ or by 266 ± 31% vs short ACh, $n = 7$ correspondingly; Fig. 1B, D). Nevertheless the amplitude of SOCE-related $[Ca^{2+}]_{cyt}$ transient produced by ACh in the presence of TG was similar to that induced by prolong application of ACh alone ($p>0.3$; Fig. 2A, C). The aforementioned stimulation protocols changed the initial slope of $[Ca^{2+}]_{cyt}$ transients in a similar manner (Fig. 2A–C). The initial slope is believed to be a more accurate reflection of the number of open SOCs [19]. The amplitude of SOCE-mediated $[Ca^{2+}]_{cyt}$ transient linearly correlates with its initial slope in all patterns of ER depletion (Fig. 2B), suggesting an increase in the number of active SOCs in the condition of a potent and prolonged stimulus.

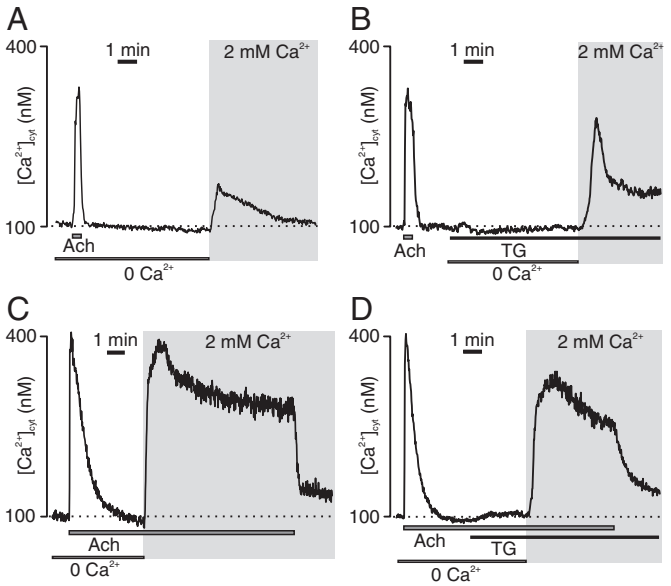

Fig. 1. Type and duration of stimulation determines the potency of SOCE. Representative recording of $[Ca^{2+}]_{cyt}$, where the ER was depleted in Ca^{2+}-free extracellular solution by a short ACh application (A), SERCA inhibitor TG (B), long application of ACh (C) or both ACh and TG in combination (D). Duration of a drug application is indicated by boxes. Following ER depletion acini were perfused with Ca^{2+} containing extracellular media to activate SOCE; duration of the perfusion is indicated by a shadowed area.

The recovery of SOCE-mediated $[Ca^{2+}]_{cyt}$ transients also depended on the stimulation protocol. Complete recovery of $[Ca^{2+}]_{cyt}$ transient was observed only when SOCE was induced by a short ACh application (Fig. 1A). The time-course of $[Ca^{2+}]_{cyt}$ recovery in TG-treated cells was biexponential, comprising fast and slow components, although we did not observe a complete recovery in the presence of extracellular Ca^{2+} (Fig. 1B). In the continuous presence of ACh, SOCE-mediated $[Ca^{2+}]_{cyt}$ transients showed only small and slow decay (Fig. 1C, D). We found no significant difference between the recovery of SOCE-mediated $[Ca^{2+}]_{cyt}$ transients induced in the continuous presence of ACh or ACh with TG (Fig. 2D). Therefore SERCA activity does not significantly influence Ca^{2+} clearance in the presence of ACh suggesting a rearrangement of the mechanisms contributing to ER refilling.

3.2. Inhibition of mitochondrial Ca^{2+} uptake and release suppresses SOCE

A crucial role of mitochondria in maintaining SOCE has been highlighted in many cell types [19,24,34]. To test an involvement of mitochondria in regulation of SOCE in the acinar cells, we run the abovementioned protocols in the presence of inhibitors of mitochondrial Ca^{2+} transport.

In line with our previous findings [17], an inhibition of mitochondrial Ca^{2+} uptake by protonophore FCCP (2 μM) induced a small and non-transient rise of $[Ca^{2+}]_{cyt}$ reflecting slow release of Ca^{2+} from mitochondria; next re-addition of extracellular Ca^{2+} produced SOCE (Fig. 3A). To exclude the potential inhibitory effect of FCCP on ATP depletion, the same experiment was performed in the presence of inhibitors of mitochondrial respiratory complex III (antimycin A, 10 mg/ml) and mitochondrial ATP synthase (oligomycin, 1 mg/ml). As shown in Fig. 3A, the effect of antimycin A and oligomycin mixture either on the release of Ca^{2+} from mitochondria or on SOCE was similar to that induced by FCCP. The inhibition of mitochondrial Ca^{2+} uptake significantly decreased both the peak amplitude and initial slope of SOCE-mediated $[Ca^{2+}]_{cyt}$ transients; such decreases were observed for all ER depletion protocols and depended on the potency of depletion (Fig. 3F). In particular, in the presence of FCCP, SOCE produced by a short ACh application was reduced by 44 ± 2% ($n = 5$, $p < 0.01$), TG—by 72 ± 9% ($n = 15$, $p < 0.01$), prolong ACh application—by 75 ± 4% ($n = 5$, $p < 0.01$), ACh with TG—by 70 ± 2% ($n = 5$, $p < 0.01$). The reduction of the initial slope of SOCE-induced $[Ca^{2+}]_{cyt}$ elevation produced by a short ACh application equaled 63 ± 12% ($n = 5$, $p < 0.01$); TG—by 80 ± 12% ($n = 10$, $p < 0.01$), prolong ACh stimulation —by 86 ± 19 ($n = 5$, $p < 0.001$), and ACh with TG—by 81 ± 15 ($n = 5$, $p < 0.01$). These results indicate the crucial role of mitochondria in providing a necessary number of open SOCs, likely by relieving their Ca^{2+}-dependent inactivation [13].

The fact that an inhibition of mitochondrial Ca^{2+} uptake equalized the amplitudes and kinetics of SOCE in all protocols indicates that mitochondria are responsible for the differences in the degree of Ca^{2+} entry. Furthermore, the contribution of mitochondrial Ca^{2+} uptake in supporting SOCE turns out to be significantly larger under prolonged stimulation.

Since Ca^{2+} uptake into mitochondria is followed by a Ca^{2+} release via NCX, we tested its contribution to SOCE. Similar to the effect of inhibition of mitochondrial Ca^{2+} uptake, the inhibition of NCX by a selective antagonist CGP 37157 (20 μM) decreased the amplitude and decelerated SOCE-mediated $[Ca^{2+}]_{cyt}$ transients in all store depletion modes with the strongest effect in the case of prolonged ER depletion protocol (Fig. 3). Contrary to FCCP, CGP 37157 did not equalize either SOCE amplitudes or kinetics. In particular, it had a less pronounced effect on the amplitude of SOCE triggered by prolong ACh application (by 52 ± 3%, $n = 6$, $p < 0.0001$; Fig. 3D, F) and insignificantly inhibited SOCE after short ACh stimulation (by 24 ± 1%, $n = 18$, $p > 0.05$; Fig. 3A–B, F). In the presence of TG or TG with ACh, the NCX blockade suppressed SOCE by 52 ± 6% ($n = 11$, $p < 0.0$; Fig. 3C, F) and 75 ± 19% ($n = 5$, $p < 0.01$; Fig. 3E, F), respectively. The initial slope of SOCE was also reduced by CGP 37157 (short Ach application: by 39 ± 4%, $n = 20$, $p < 0.05$; TG: by 76 ± 8%, $n = 12$, $p < 0.01$; prolonged Ach: by 47 ± 7%, $n = 6$, $p < 0.01$; ACh with TG: by 69 ± 9%, $n = 8$, $p < 0.01$; Fig. 3B–F).

These data indicate that mitochondrial Ca^{2+} buffering capacity is sufficient to avoid Ca^{2+}-dependent inactivation of SOCE induced by a short stimulation, while trans-mitochondrial transport is essential for supporting SOCE under sustained stimulation.

3.3. Mitochondrial $[Ca^{2+}]$ dynamics following SOCE activation

To directly monitor Ca^{2+} dynamics in mitochondria during SOCE, we measured $[Ca^{2+}]_{mit}$ changes in rhod-2-loaded cells (Fig. 4A–B, upper panel). The activation of SOCE following a short ACh application yielded a small increase of $[Ca^{2+}]_{mit}$ (Fig. 4A, lower panel), whereas prolong ACh stimulation, TG or both caused a large $[Ca^{2+}]_{mit}$ rise (Fig. 4B, C). The amplitudes of SOCE-induced $[Ca^{2+}]_{mit}$ transients triggered by TG were increased by 126 ± 17% ($n = 9$, $p < 0.05$), ACh with TG—by 400 ± 62% ($n = 5$, $p < 0.01$) and continuous present ACh—by 506 ± 67% ($n = 7$, $p < 0.001$) versus short ACh (Fig. 4E). We found that the initial slope of SOCE-mediated $[Ca^{2+}]_{cyt}$ transient positively correlates with the initial slope of $[Ca^{2+}]_{mit}$ rise for all ER depletion protocols (Fig. 4D). The latter further supports the idea that accelerated mitochondrial Ca^{2+} accumulation serves to relieve Ca^{2+}-dependent desensitization of SOCs under potent stimulation. In separate control experiments, we demonstrated a drop of $[Ca^{2+}]_{mit}$ after application of FCCP that represents release of Ca^{2+} from mitochondria consistently with our previous observations [17]; any $[Ca^{2+}]_{mit}$ rise was observed after re-addition of extracellular Ca^{2+} in the conditions of inhibited mitochondrial Ca^{2+} uptake (Fig. 4A, lower panel). At the same time, activation of SOCE in the presence of CGP resulted in a transient rise of $[Ca^{2+}]_{mit}$ and no recovery of $[Ca^{2+}]_{mit}$ was observed while CGP was present (Fig. 4B), confirming that NCX is a sole route for Ca^{2+} release from the mitochondria.

To probe for a functional proximity of mitochondrial Ca^{2+} uptake sites and SOCs in the plasma membrane, we compared the effects of slow (EGTA) and fast (BAPTA) Ca^{2+} buffers added to the intrapipette solution on the SOCE-induced changes of $[Ca^{2+}]_{mit}$. EGTA is not effective for buffering Ca^{2+} microdomains, whereas BAPTA effectively buffers short-

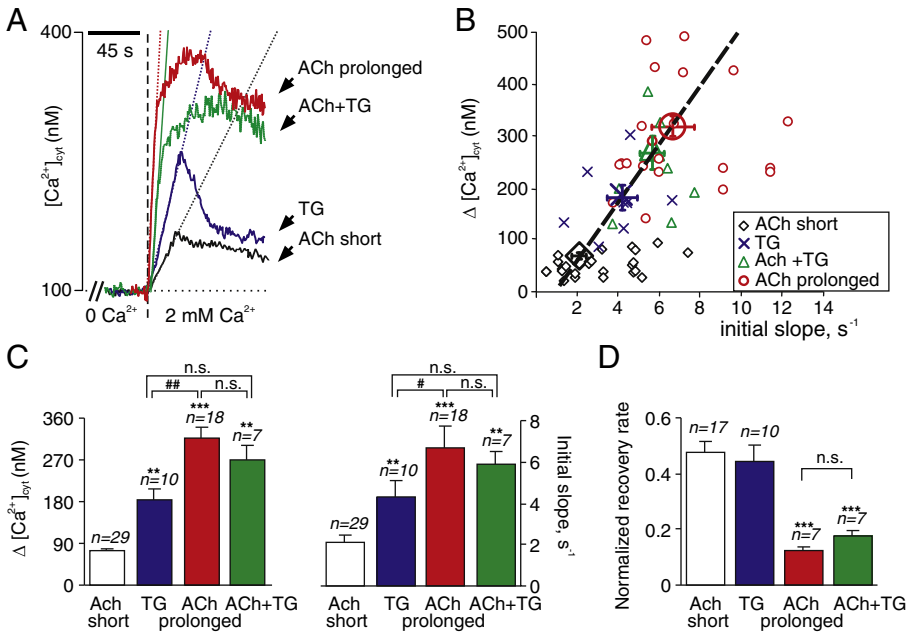

Fig. 2. The slope of SOCE-mediated $[Ca^{2+}]_{cyt}$ transients correlates with the degree of ER depletion. Kinetic and amplitude profiles of SOCE for all patterns of ER depletion tested (A). Dotted lines represent the initial slope of $[Ca^{2+}]_{cyt}$ transients. A scatter plot of amplitudes of SOCE-induced $[Ca^{2+}]_{cyt}$ transients plotted against their initial slopes for different stimulation protocols (B). The bigger symbols are the mean values for the corresponding dataset. Statistical analysis of amplitude and initial slope of SOCE (C). Normalized recovery rate of SOCE-induced $[Ca^{2+}]_{cyt}$ transients (D). $^{*}p<0.05$, $^{**}p<0.01$ versus ACh short; $^{\#}p<0.05$, $^{\#\#}p<0.01$ versus indicated series.

lived Ca^{2+} microdomains because of faster binding kinetics [20]. The SOCE-mediated $[Ca^{2+}]_{mit}$ elevation induced by a short ACh application was not significantly different in cells perfused with either BAPTA or EGTA ($\Delta F/F_0$ was 0.137 ± 0.040 versus 0.197 ± 0.043, $n=5$, $p>0.1$; Fig. 5A, C). By contrast, in the continuous ACh presence, BAPTA suppressed and decelerated SOCE-mediated $[Ca^{2+}]_{mit}$ transients by $52\pm8\%$ ($n=6$, $p<0.01$) and $40\pm4\%$ ($n=5$, $p<0.05$; Fig. 5B, C). These findings directly indicate a formation of microdomains of high Ca^{2+} between mitochondria uptake sites and SOCs during sustained stimulation.

3.4. Mitochondria control intra-ER Ca^{2+} dynamics

To confirm the fact that both the amplitude and kinetics of SOCE-induced $[Ca^{2+}]_{cyt}$ and $[Ca^{2+}]_{mit}$ transients depend on the type and duration of ER depletion, one needs to perform direct measurements of luminal Ca^{2+} dynamics and estimate the levels of ER depletion/refilling. For this we used a low-affinity Ca^{2+} dye mag-fura-2. Short ACh stimulation in Ca^{2+}-free solution produced a modest significant transient decrease in $[Ca^{2+}]_{ER}$ ($\Delta F_{340}/F_{380}$ ratio was decreased by 0.030 ± 0.003, $n=18$; Fig. 6A). Re-addition of extracellular Ca^{2+} after a short ACh application initiated ER refilling, which was biexponential with initial fast and subsequent slow components and accomplished within 5 min (Fig. 6A). Prolonged ACh stimulation triggered pronounced $[Ca^{2+}]_{ER}$ decrease (by 0.097 ± 0.008, $n=10$; Fig. 6A), which, upon Ca^{2+} re-addition, was followed by ER refilling. The normalized initial rate of ER refilling was $181\pm30\%$ faster compared to that after a short ACh ($n=10$, $p<0.01$). The ER refilling was never fully accomplished in the presence of ACh, which reflects continuous $InsP_3$-induced Ca^{2+} release from the ER. The very similar kinetics of ER depletion and refilling was also recorded when the intrapipette solution contained 10 μM of $InsP_3$ (data not shown). In a separate group of control experiments, we demonstrated no recovery of $[Ca^{2+}]_{ER}$ upon activation of SOCE in the presence of TG or TG with ACh (Fig. 6A). We found the linear correlation between the initial slopes of SOCE-induced $[Ca^{2+}]_{cyt}$ transients and the integrated $\int[Ca^{2+}]_{ER}(t)$ function over the duration of stimulation for all protocols (Fig. 6D). The integrated $\int[Ca^{2+}]_{ER}(t)$ was proportional to the amount of calcium released from the ER. This suggests that stronger stimulation produces the larger ER depletion as well as larger SOCE activation with an increased number of active SOCs.

Since the inhibition of NCX decreases and decelerates SOCE-induced $[Ca^{2+}]_{cyt}$ transients, we hypothesized that Ca^{2+} released by mitochondria should contribute to the ER refilling. We suggested also that an increased effect of CGP 37157 on SOCE induced by a prolonged ACh stimulation might reflect the larger impact of Ca^{2+} released by mitochondria to the ER refilling. We found that in mag-fura-2/AM-loaded cells after short administration of ACh with CGP 37157, the efficacy of ER refilling decreased by $30\pm7\%$ ($n=14$, $p<0.01$) with no significant changes of its initial slope (Fig. 6B). However, in the continuous presence of ACh, CGP 37157 caused both dramatic inhibition of SOCE-mediated ER refilling (by $78\pm14\%$, $n=10$, $p<0.001$) and its deceleration (by $59\pm21\%$, $n=9$, $p<0.01$; Fig. 6C). These results demonstrate the increased contribution of mitochondrial Ca^{2+} release to the ER refilling in the conditions of prolonged cell stimulation.

We further tested the role of NCX in the ER refilling using fura-2/AM-loaded cells stimulated by short or prolonged ACh applications. We first stimulated cells with ACh to activate SOCE and then allowed the ER to refill in the absence or presence of CGP 37157. Subsequently ACh was applied for the second time in the Ca^{2+} free media. The amplitude of second ACh-induced $[Ca^{2+}]_{cyt}$ transient was then used as a measure of the amount of Ca^{2+} accumulated in the ER being hence the readout of the efficacy of ER refilling. We found that when ER was refilled in the absence of ACh, CGP 37157 resulted in a decreased amplitude of second ACh-induced $[Ca^{2+}]_{cyt}$ transient by $32\pm6\%$ ($n=15$, $p<0.001$; Fig. 5E). When NCX was inhibited and ACh was present during Ca^{2+} re-addition, the second ACh-induced $[Ca^{2+}]_{cyt}$ transient was almost completely abolished ($88\pm7\%$ reduction, $n=15$, $p<0.001$; Fig. 5F). These data further demonstrate that under prolonged agonist stimulation, Ca^{2+} release from mitochondria represents a major pathway for the ER refilling.

3.5. The ability of mitochondria to allocate store-operated Ca^{2+} influx and define the pattern of ER refilling is due to their specific subcellular localization

Our data suggest the several physical limitations on a localization of intracellular organelles: (i) mitochondria should be closely

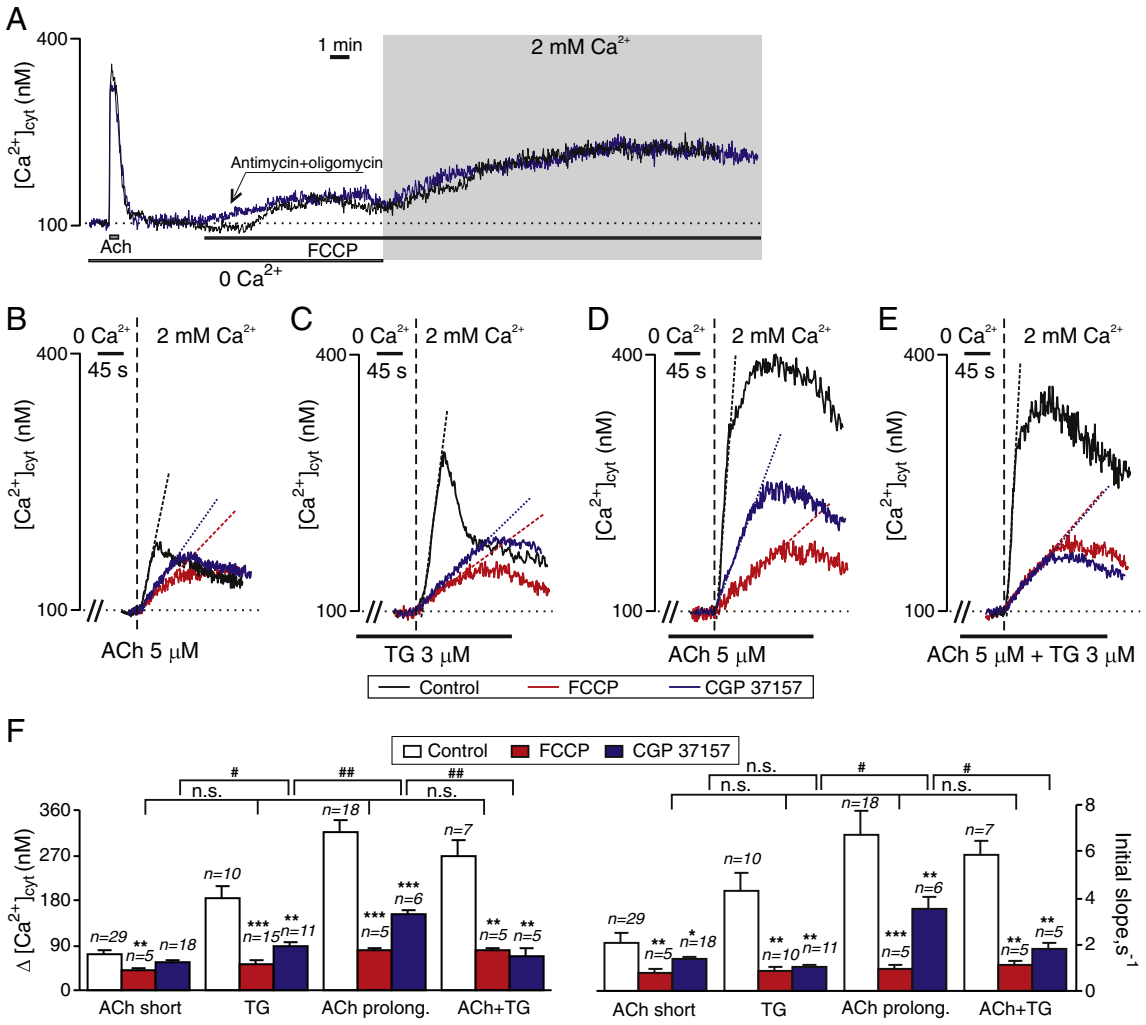

Fig. 3. Mitochondrial Ca^{2+} uptake and release via NCX is required for sustained SOCE. An overlay of representative recordings of $[Ca^{2+}]_{cyt}$, where the ER was first depleted in Ca^{2+}-free extracellular solution by a short ACh application with following Ca^{2+} re-addition in the presence of FCCP (black trace) or mixture of antimycin and oligomycin (blue trace) (A). An overlay of SOCE-induced $[Ca^{2+}]_{cyt}$ transients before, after FCCP or CGP 37157 applications (B–E). Statistical analysis of amplitudes and initial slopes of SOCE with or without FCCP or CGP 37157 (F). $^{*}p<0.05$, $^{**}p<0.01$, $^{***}p<0.001$ versus control, $^{\#}p<0.05$, $^{\#\#}p<0.01$ versus indicated series.

associated with ER to enable formation of Ca^{2+} microdomains; (ii) mitochondria should be close to PM to prevent Ca^{2+} dependent inactivation of SOCE; (iii) ER should be close to PM to allow the direct (bypassing the cytoplasm) and efficient ER refilling. The availability of the conditions outlined in (i) and (ii) were in part shown earlier [17], when we described two groups of mitochondria: first, close to ER membrane around the nucleus (peri-reticulum mitochondria), and the second, adjacent to PM (subplasmalemmal mitochondria). There were no ER strands between the PM and subplasmalemmal mitochondria while ER surrounded it on the other side. To support the existence of the conditions iii) and to further clarify a mitochondria location relative to other organelles, we performed an EM analysis of the internal structure of basolateral region of submandibular acinar cell. We measured the percentage of the PM directly opposed by either mitochondria or the ER; the shortest distance between the PM and ER as well as the PM and mitochondria; the ratio of the total number of subplasmalemmal mitochondria to the number of mitochondria localized within 10 nm from the PM.

Using 100 EM images obtained from 10 cells we found that the ER occupied $21\pm3\%$ and mitochondria $23.5\pm4\%$ of space directly beneath basolateral PM. The shortest distance between the ER and PM was in average 23 ± 2 nm ($n=61$ strands of ER in 8 cells); in some cases it was less than 7 nm (Fig. 7C). The shortest distance between the mitochondria and the PM was in average 26 ± 3 nm ($n=69$ mitochondria in 9 cells); it was as small as 6 nm (Fig. 7B). The ratio of mitochondria lying in the closest vicinity of PM (less 10 nm) to the total number of subplasmalemmal mitochondria was $67\pm3\%$. These EM data support the physical requirements outlined in (i), (ii), (iii) corroborating the existence of two ER refilling mechanisms.

4. Discussion

During the tasting and chewing food the frequency of ACh release substantially increases, causing up to ten-fold increase in salivation. The maintenance of an efficient fluid and protein saliva secretion in the conditions of prolonged presence of an agonist requires (i) dynamic interaction between Ca^{2+} release and Ca^{2+} influx sites to preserve Ca^{2+}-dependent K^+ and Cl^- channels activity for the prolonged period of time; (ii) an effective refilling of the ER, since a proper $[Ca^{2+}]_{ER}$ level is essential for a proteins processing and secretion [5], (iii) an effective buffering of Ca^{2+} entering acinar cells to prevent Ca^{2+}-dependent inactivation of SOCs [13,14] and cytoplasmic Ca^{2+} overload to limit Ca^{2+} toxicity. Therefore, acinar cells require specific mechanisms adapting Ca^{2+}-regulating machinery under sustained stimulation to ensure the efficiency of secretion at the same time avoiding risks of cytoplasmic Ca^{2+} overload and ER

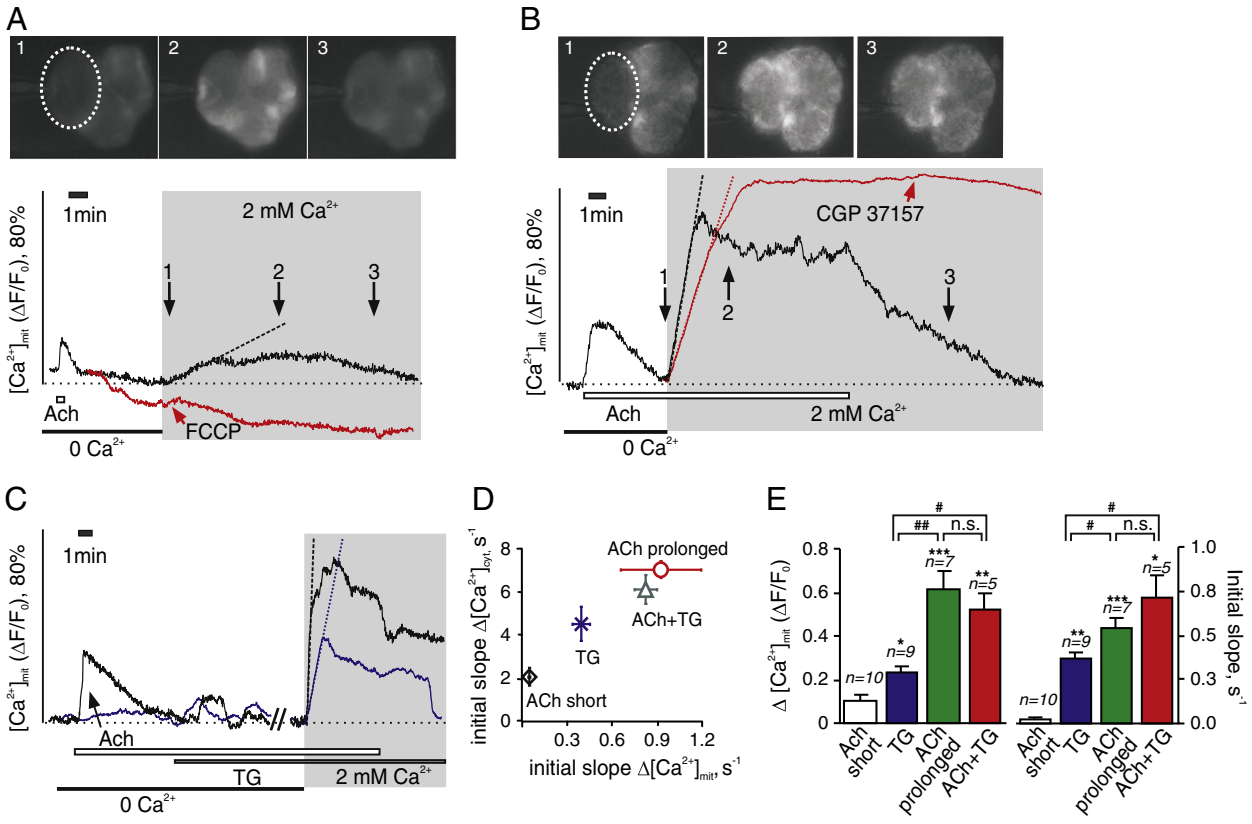

Fig. 4. SOCE-mediated $[Ca^{2+}]_{mit}$ transients are proportional to stimulation potency. A representative recording of changes in $[Ca^{2+}]_{mit}$ during a short application of ACh in Ca^{2+}-free extracellular solution followed by Ca^{2+} re-addition (A, lower panel); red trace is recording of $[Ca^{2+}]_{mit}$ in the presence of FCCP. Rhod-2 fluorescent images of patch-clamped cell triplet, acquired at the time points indicated in lower panel (A, upper panel). Experiment same to (A) except that SOCE was activated by prolonged ACh application (B). Red trace is SOCE-induced $[Ca^{2+}]_{mit}$ signal in the presence of CGP 37157. SOCE-mediated $[Ca^{2+}]_{mit}$ transients following ER depletion with either TG or TG with ACh (C). A scatter plot of $[Ca^{2+}]_{cyt}$ transients initial slope against $[Ca^{2+}]_{mit}$ initial slope for indicated protocols (D). Statistical analysis of amplitudes and initial slopes of SOCE-induced $[Ca^{2+}]_{mit}$ transients (E). $^{*}p<0.05$, $^{**}p<0.01$, $^{***}p<0.001$ versus ACh short; $^{\#}p<0.05$, $^{\#\#}p<0.01$ versus indicated series.

depletion. Here we show that these mechanisms include the rearrangement of intracellular Ca^{2+} sequestration and an increased role of trans-mitochondrial Ca^{2+} transport within the cell.

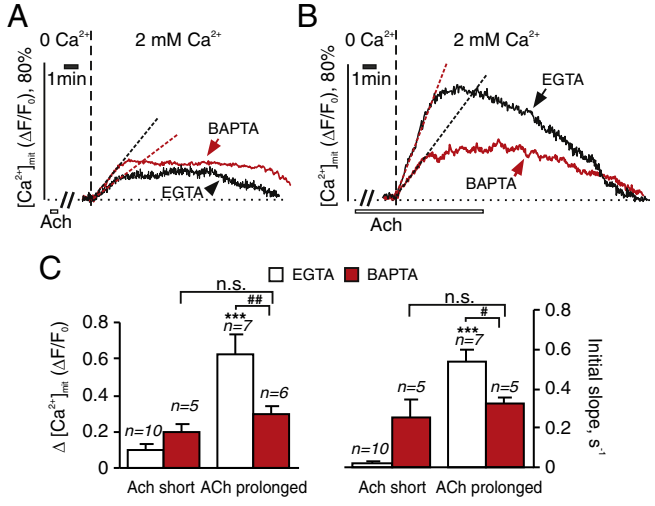

Fig. 5. Rise in $[Ca^{2+}]_{mit}$ under SOCE activation occurs via Ca^{2+} microdomains, but only during sustained stimulation. An overlay of SOCE-induced $[Ca^{2+}]_{mit}$ transients following a depletion of the ER with short application of ACh in the presence of EGTA- or BAPTA-containing Ca^{2+} buffer (A). Experiment same to (A) except that SOCE was activated by prolonged ACh application (B). Statistical analysis of the effects of EGTA and BAPTA on amplitudes and initial slopes of $[Ca^{2+}]_{mit}$ transients (C). $^{**}p<0.01$ versus ACh short, $^{\#\#}p<0.01$ versus indicated series.

SOCE is an intrinsic component of an agonist-induced response, crucial for the prolongation and regeneration of Ca^{2+} transients, and ultimately the secretion [7]. To temporally separate SOCE from an $InsP_3$-dependent release from the ER and investigate SOCE dependence on a stimulation pattern, we used an approach in which ER depletion was followed by the re-addition of extracellular Ca^{2+} [19,21]. The amplitudes and more importantly slopes [19] of SOCE-mediated $[Ca^{2+}]_{cyt}$ transients strongly correlated with the degree of ER depletion (Figs. 2B,C, 6D), showing that increased ER depletion translates to the increased number of active SOCs. It may represent a bigger proportion of STIM1 translocation to the PM during stronger ER depletion and forming more TRP1–STIM1–Orai1 complexes in the lipid raft domains [9,11]. Besides, the maintenance of robust SOCE under sustained stimulation suggests the presence of an adaptation mechanism preventing Ca^{2+}-dependent inactivation of SOCs [22,23].

In the continuous presence of ACh, the recovery of SOCE-induced $[Ca^{2+}]_{cyt}$ transients was much slower compared to either a short application of ACh or TG alone (Fig. 2D). It suggests that during a prolonged presence of an agonist there is an additional Ca^{2+} release from an intracellular compartment. We reasoned that this is mitochondria taking up Ca^{2+} during SOCE and interacting with other Ca^{2+} sequestrating systems, such as SERCA, in the manner that depends on the presence of an agonist. Indeed, there is a substantial body of evidence describing an ability of mitochondria to influence ER-dependent Ca^{2+} entry [15,19,24], however, their contribution to SOCE maintenance in acinar cells is unknown yet. The acinar cells have unique Ca^{2+} signaling machinery specifically adapted to their structural and functional polarization [2,4,25]. In highly polarized acinar cells, extremely developed rough ER is localized in basolateral

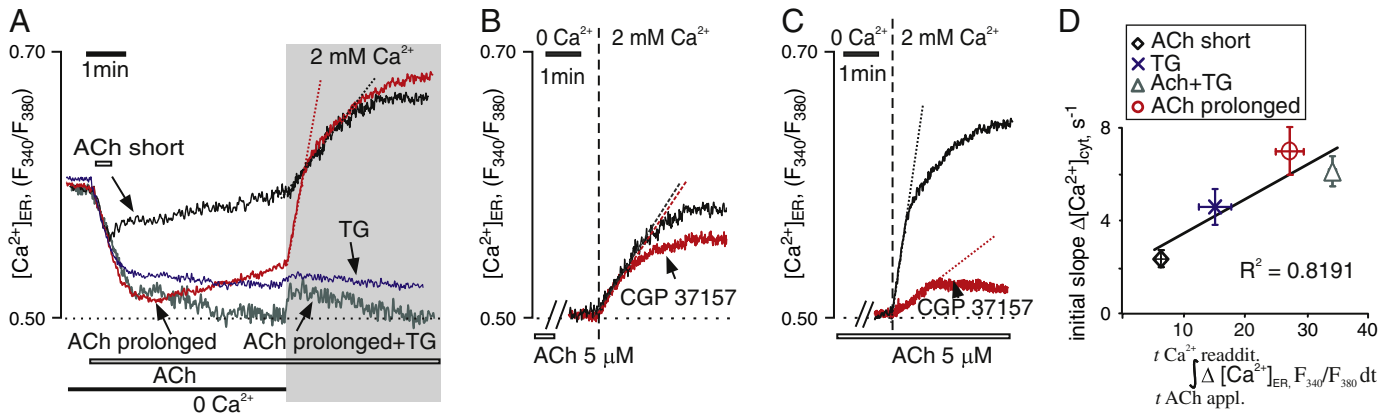

Fig. 6. Stimulation pattern defines the mechanism of ER refilling. An overlay of $[Ca^{2+}]_{ER}$ traces demonstrating ER refilling following a short or prolonged ACh, TG or ACh and TG in patched cells (A). Dotted lines represent the initial rate of ER refilling where SERCAs were available. Effect of CGP 37157 on SOCE-induced ER refilling following short or prolonged ACh application (B, C). The relationship between the initial slopes of SOCE-induced $[Ca^{2+}]_{cyt}$ transients and the measure of ER depletion (integrated $[Ca^{2+}]_{ER}(t)$ function) for different stimulations.

cell regions as well as the abundant mitochondria are colocalized in close vicinity with PM and ER [4,17,26].

Our results demonstrated that mitochondria are required for the maintaining of SOCE in all ER depletion protocols. Blocking of mitochondrial Ca^{2+} uptake equalized the amplitudes and slopes of SOCE transients (Fig. 3), indicating that mitochondria are responsible for the differences in the degree of SOCE activation. Furthermore, there is a positive correlation between the number of open SOCs and the rate of $[Ca^{2+}]_{mit}$ transients (Fig. 4D). Several possible mechanisms have recently been implicated to explain the ability of mitochondria to facilitate SOCE. Mitochondria can reduce Ca^{2+}-dependent inactivation of SOCs buffering cytoplasmic Ca^{2+} in the ER–PM junctions, thus maintain the channel's activity [22,23]. The rise in $[Ca^{2+}]_{mit}$ potentiates ATP synthesis and aerobic metabolism [15]. An increase in local ATP can either energize nearby Ca^{2+} pumps or ATP can serve as a Ca^{2+} buffer itself [27,28]. In addition, pyruvic acid, a key metabolic product of mitochondria, directly reduces SOCs inactivation independently of mitochondrial Ca^{2+} uptake or ATP production [29]. Although we cannot pinpoint the exact mechanism by which mitochondrial facilitate SOCE, our results strongly argue for a pivotal role of mitochondria in maintaining of SOCE.

We also showed that mitochondrial Ca^{2+} uptake sites are closely opposing the Ca^{2+} entry sites on the PM forming microdomains of high $[Ca^{2+}]$ since fast Ca^{2+} chelator BAPTA was more effective in limiting mitochondrial Ca^{2+} uptake during SOCE compared to EGTA (Fig. 5). This suggests that the distance between the SOC mouth and mitochondrial uptake site has to be between ~10 and 90 nm, as was estimated previously [20,27]. The formation of Ca^{2+} microdomains occurs only in the continuous presence of an agonist, suggesting the saturation of subplasmalemmal SERCA in the condition when powerful SOCE exceeds their pumping ability; the effect recognized in other cell types [30]. Therefore, during a potent stimulation the cell adapts its Ca^{2+} clearance system directing more Ca^{2+} into mitochondria.

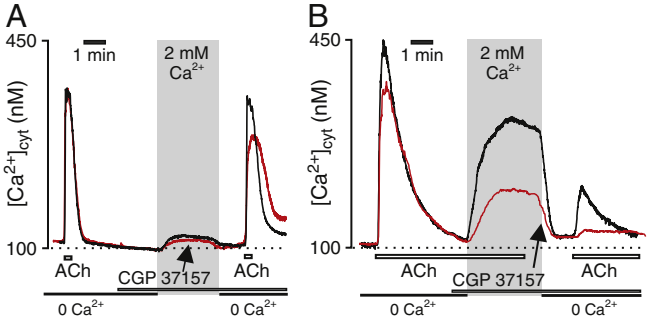

Fig. 7. Stimulation pattern defines the mechanism of ER refilling. An overlay of representative $[Ca^{2+}]_{cyt}$ responses in intact cells evoked by two ACh applications in Ca^{2+}-free media intermitted by the re-addition of Ca^{2+} (enabling the ER refilling) in the presence or absence of CGP 37157 (A). The amplitude of second ACh-induced $[Ca^{2+}]_{cyt}$ transient was used as an indicator of the effectiveness of ER refilling. Experiment similar to (A) except that ACh was continuously present during ER refilling (B).

Mitochondrial Ca^{2+} accumulation reflects the efficacy of two processes: Ca^{2+} uptake and Ca^{2+} release [28]. By measuring $[Ca^{2+}]_{mit}$ we show that NCX is a sole route for Ca^{2+} release from the mitochondria (Fig. 4B). However, contrary to blocking mitochondrial Ca^{2+} uptake, an inhibition of NCX did not change SOCE induced by a short ACh suggesting that intrinsic Ca^{2+} buffering capacity of mitochondria is sufficient to prevent initial inactivation of SOCE. On the other hand, in the continuous presence of an agonist, an inhibition of NCX significantly reduced SOCE, representing the gradual (within minutes) SOCs inactivation caused by the inability of mitochondria to take up more Ca^{2+} due to eliminated residual Ca^{2+} release through NCX. The latter is likely explained by an increased acidification of mitochondria matrix and uniporter inactivation [29]. Ca^{2+} release through NCX may represent an additional source for the ER refilling. Involvement of NCX in the ER refilling was quantified by two approaches: (i) direct measurement of $[Ca^{2+}]_{ER}$ replenishment; (ii) comparison of the amount of Ca^{2+} released from the ER by ACh before and after the ER refilling. During a short ACh application the blockade of NCX diminished ER refilling and decreased the amount of releasable Ca^{2+} inside the ER by ~30% (Fig. 6E). Ca^{2+} released by NCX is taken up into the ER by SERCA via microdomains of high local $[Ca^{2+}]$, since CGP 37157 did not affect the amplitude of SOCE (Fig. 3A, E). Our EM data support this conclusion revealing a close spatial proximity of mitochondria and ER membranes (Fig. 7) along with such observations in other cell types [14,31]. Hence, in the absence of an agonist, the bulk of Ca^{2+} entering the acinar cell during SOCE is rapidly accumulated into the ER by SERCA without a robust increase in $[Ca^{2+}]_{cyt}$ (Fig. 8A). Direct SERCA-mediated ER refilling is possible because of tight macromolecular assembly of TRPC1 and Orai1 with STIM1 within ER–plasma membrane lipid raft domains and their colocalization with other Ca^{2+} sensitive proteins (e.g. SERCA, PMCA, PLC, $InsP_3$ receptors) involved in an activation of SOCs [10,32,33]. Due to our data (see also [26]) close apposition of the ER strands and the PM ensures a formation of the microdomains of high $[Ca^{2+}]$.

In the absence of an agonist, we did not observe Ca^{2+}-dependent inactivation of SOCs because SERCAs provide sufficient pumping (see also [24,34]). In the continuing agonist presence, the close apposition of the PM and ER will put a strain on the prolonged functioning of

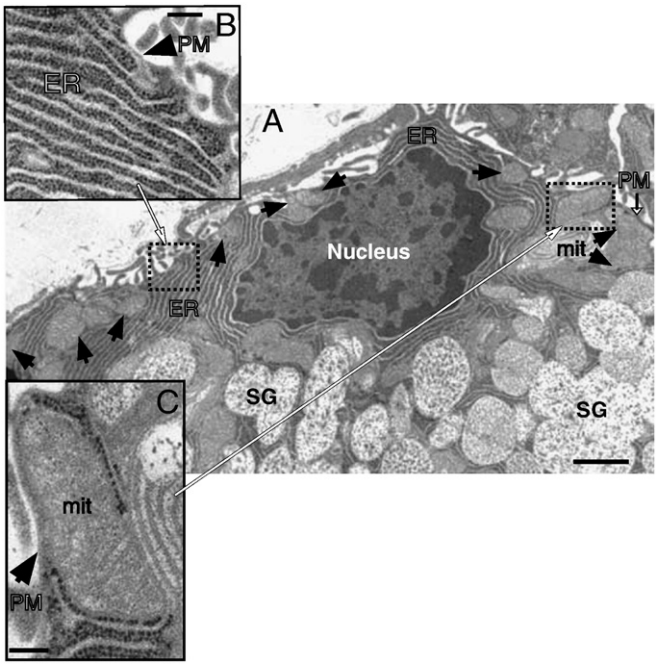

Fig. 8. Relative positions of mitochondria, ER and PM in the basolateral region of acinar cell. An electron-microscopy image of intracellular structure of the basolateral region of acinar cell (SG, secretory granules; mit, mitochondrion) (A). Scale bar = 1 μm. A representative example of the ER strands establishing close contacts with PM in the basolateral region of cell (B). An example of the close association between a mitochondrion and PM (C). Scale bars = 0.1 μm.

SOCs because of constant Ca^{2+} release through subplasmalemmal $InsP_3$ receptors leads to saturation of nearby SERCAs and Ca^{2+}-dependent inactivation of SOCs. Indeed, overlapping localization of

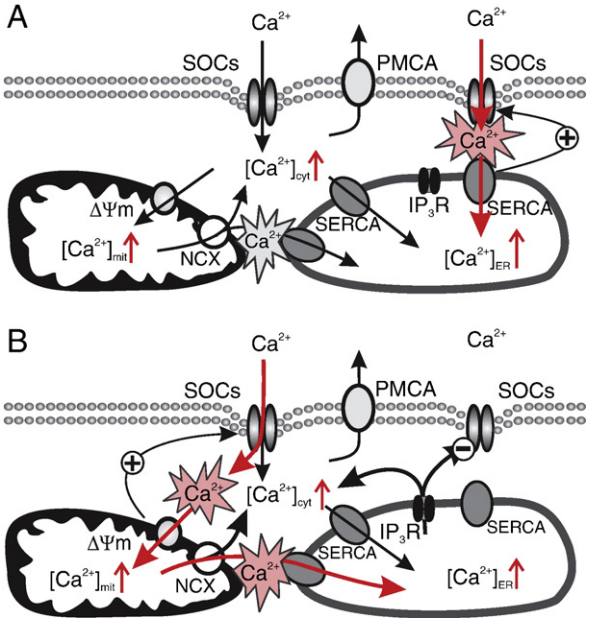

Fig. 9. Proposed model for an adaptation of Ca^{2+} signaling to a pattern of agonist stimulation. In the absence of an agonist, the bulk of Ca^{2+} entering the cell following SOCE does not spread into cytosol and is sequestered into the ER via subplasmalemmal SERCA preventing Ca^{2+}-dependent inactivation of SOCs (positive feedback) (A). When an agonist is present during SOCE, Ca^{2+} outflow constantly from the ER through $InsP_3$ receptors that leads to a saturation of subplasmalemmal SERCAs and SOCs inactivation (negative feedback) (B). Mitochondria relieve Ca^{2+}-inactivation of SOCs taking up Ca^{2+}, tunneling and subsequently releasing through NCX (positive feedback). Stars indicate microdomains of high local $[Ca^{2+}]$.

$InsP_3$ receptors and SERCAs has been demonstrated in the basolateral part of acinar cells [35,36]. Moreover, $InsP_3$ receptors can relocate into the punctae of the subplasmalemmal region upon the ER depletion [37] facilitating Ca^{2+}-dependent inactivation of SOCs. Therefore, under the sustained stimulation, the maintenance of SOCE is only possible due to the involvement of additional system, which recedes Ca^{2+} away from the PM preventing the inactivation of SOCs. Our data suggest that mitochondria play this role in acinar cells being located in the vicinity of the PM and providing a tunneling of Ca^{2+} further away from the PM (Fig. 9). The existence of trans-mitochondrial Ca^{2+} diffusion was demonstrated in other cell types [34,38]. Such diffusion follows a formation of high local $[Ca^{2+}]$ domains inside mitochondria in the conditions unfavorable for Ca^{2+} extrusion and provides Ca^{2+} transport to the extrusion sites distal from Ca^{2+} uptake. In the conditions of sustained stimulation, such extrusion is crucial for the ER refilling, since Ca^{2+} sequestered into the mitochondria within the PM-mitochondria junctions diffuses through the mitochondria and is redirected to the unsaturated SERCAs away from the PM (Fig. 8B).

In conclusion, (i) activation of SOCE is associated with the increases in $[Ca^{2+}]_{cyt}$, $[Ca^{2+}]_{mit}$ and $[Ca^{2+}]_{ER}$, which amplitude and kinetic correlate with the degree of ER depletion; (ii) in the absence of an agonist, the ER refilling occurs mainly through SERCA-mediated Ca^{2+} uptake within ER–PM junctions; (iii) under the sustained stimulation, mitochondria are the core system responsible for the sustained SOCE and sufficient ER refilling. The ability of mitochondria to adjust Ca^{2+} dynamic to the pattern of cell stimulation may represent a novel function of mitochondria as an intrinsic adaptation mechanism enabling a long-lasting secretion.

References

[1] I.S. Ambudkar, Regulation of calcium in salivary gland secretion, Crit. Rev. Oral Biol. Med. 11 (2000) 4–25.
[2] J.E. Melvin, D. Yule, T. Shuttleworth, T. Begenisich, Regulation of fluid and electrolyte secretion in salivary gland acinar cells, Annu. Rev. Physiol. 67 (2005) 445–469.
[3] J.E. Melvin, L. Koek, G.H. Zhang, A capacitative Ca^{2+} influx is required for sustained fluid secretion in sublingual mucous acini, Am. J. Physiol. 261 (1991) 1043–1050.
[4] O. Larina, P. Thorn, Ca^{2+} dynamics in salivary acinar cells: distinct morphology of the acinar lumen underlies near-synchronous global Ca^{2+} responses, J. Cell Sci. 118 (2005) 4131–4139.
[5] A. Verkhratsky, Physiology and pathophysiology of the calcium store in the endoplasmic reticulum of neurons, Physiol. Rev. 85 (2005) 201–279.
[6] X. Liu, B.B. Singh, I.S. Ambudkar, TRPC1 is required for functional store-operated Ca^{2+} channels. Role of acidic amino acid residues in the S5–S6 region, J. Biol. Chem. 278 (2003) 11337–11343.
[7] X. Liu, K.T. Cheng, B.C. Bandyopadhyay, B. Pani, A. Dietrich, B.C. Paria, W.D. Swaim, D. Beech, E. Yildrim, B.B. Singh, L. Birnbaumer, I.S. Ambudkar, Attenuation of store-operated Ca^{2+} current impairs salivary gland fluid secretion in TRPC1(−/−) mice, Proc. Natl. Acad. Sci. U. S. A 104 (2007) 17542–17547.
[8] S.L. Zhang, Y. Yu, J. Roos, J.A. Kozak, T.J. Deerinck, M.H. Ellisman, K.A. Stauderman, M.D. Cahalan, STIM1 is a Ca^{2+} sensor that activates CRAC channels and migrates from the Ca^{2+} store to the plasma membrane, Nature 437 (2005) 902–905.
[9] K.T. Cheng, X. Liu, H.L. Ong, I.S. Ambudkar, Functional requirement for Orai1 in store-operated TRPC1-STIM1 channels, J. Biol. Chem. 283 (2008) 12935–12940.
[10] H.L. Ong, K.T. Cheng, X. Liu, B.C. Bandyopadhyay, B.C. Paria, J. Soboloff, B. Pani, Y. Gwack, S. Srikanth, B.B. Singh, D.L. Gill, I.S. Ambudkar, Dynamic assembly of TRPC1–STIM1–Orai1 ternary complex is involved in store-operated calcium influx. Evidence for similarities in store-operated and calcium release-activated calcium channel components, J. Biol. Chem. 282 (2007) 9105–9116.
[11] B. Pani, H.L. Ong, X. Liu, K. Rauser, I.S. Ambudkar, B.B. Singh, Lipid rafts determine clustering of STIM1 in endoplasmic reticulum–plasma membrane junctions and regulation of store-operated Ca^{2+} entry (SOCE), J. Biol. Chem. 283 (2008) 17333–17340.
[12] M.R. Duchen, A. Verkhratsky, S. Muallem, Mitochondria and calcium in health and disease, Cell Calcium 44 (2008) 1–5.
[13] A.B. Parekh, J.W. Putney Jr., Store-operated calcium channels, Physiol. Rev. 85 (2005) 757–810.
[14] R. Rizzuto, M.R. Duchen, T. Pozzan, Flirting in little space: the ER/mitochondria Ca^{2+} liaison, Sci. STKE. 2004 (2004) re1.
[15] J.A. Gilabert, A.B. Parekh, Respiring mitochondria determine the pattern of activation and inactivation of the store-operated Ca(2+) current I(CRAC), EMBO J. 19 (2000) 6401–6407.
[16] N.V. Fedirko, I.A. Kruglikov, O.V. Kopach, J.A. Vats, P.G. Kostyuk, N.V. Voitenko, Changes in functioning of rat submandibular salivary gland under streptozotocin-induced diabetes are associated with alterations of Ca^{2+} signaling and Ca^{2+} transporting pumps, Biochim. Biophys. Acta 1762 (2006) 294–303.

[17] O. Kopach, I. Kruglikov, T. Pivneva, N. Voitenko, N. Fedirko, Functional coupling between ryanodine receptors, mitochondria and Ca(2+) ATPases in rat submandibular acinar cells, Cell Calcium 43 (2008) 469–481.
[18] N. Solovyova, N. Veselovsky, E.C. Toescu, A. Verkhratsky, Ca(2+) dynamics in the lumen of the endoplasmic reticulum in sensory neurons: direct visualization of Ca(2+)-induced Ca(2+) release triggered by physiological Ca(2+) entry, EMBO J. 21 (2002) 622–630.
[19] M.D. Glitsch, D. Bakowski, A.B. Parekh, Store-operated Ca^{2+} entry depends on mitochondrial Ca^{2+} uptake, EMBO J. 21 (2002) 6744–6754.
[20] M. Naraghi, E. Neher, Linearized buffered Ca^{2+} diffusion in microdomains and its implications for calculation of $[Ca^{2+}]$ at the mouth of a calcium channel, J. Neurosci. 17 (1997) 6961–6973.
[21] J. Yao, Q. Li, J. Chen, S. Muallem, Subpopulation of store-operated Ca^{2+} channels regulate Ca^{2+}-induced Ca^{2+} release in non-excitable cells, J. Biol. Chem. 279 (2004) 21511–21519.
[22] A.B. Parekh, Store-operated Ca^{2+} entry: dynamic interplay between endoplasmic reticulum, mitochondria and plasma membrane, J. Physiol. 547 (2003) 333–348.
[23] A. Zweifach, R.S. Lewis, Rapid inactivation of depletion-activated calcium current (ICRAC) due to local calcium feedback, J. Gen. Physiol. 105 (1995) 209–226.
[24] R. Malli, M. Frieden, M. Trenker, W.F. Graier, The role of mitochondria for Ca^{2+} refilling of the endoplasmic reticulum, J. Biol. Chem. 280 (2005) 12114–12122.
[25] O.H. Petersen, A.V. Tepikin, Polarized calcium signaling in exocrine gland cells, Annu. Rev. Physiol. 70 (2008) 273–299.
[26] M.K. Park, M.C. Ashby, G. Erdemli, O.H. Petersen, A.V. Tepikin, Perinuclear, perigranular and sub-plasmalemmal mitochondria have distinct functions in the regulation of cellular calcium transport, EMBO J. 20 (2001) 1863–1874.
[27] G.B. Montalvo, A.R. Artalejo, J.A. Gilabert, ATP from subplasmalemmal mitochondria controls Ca^{2+}-dependent inactivation of CRAC channels, J. Biol. Chem. 281 (2006) 35616–35623.
[28] G. Szabadkai, M.R. Duchen, Mitochondria: the hub of cellular Ca^{2+} signaling, Physiology (Bethesda) 23 (2008) 84–94.
[29] D. Bakowski, A.B. Parekh, Regulation of store-operated calcium channels by the intermediary metabolite pyruvic acid, Curr. Biol. 17 (2007) 1076–1081.
[30] H. Jousset, M. Frieden, N. Demaurex, STIM1 knockdown reveals that store-operated Ca^{2+} channels located close to sarco/endoplasmic Ca^{2+} ATPases (SERCA) pumps silently refill the endoplasmic reticulum, J. Biol. Chem. 282 (2007) 11456–11464.
[31] R. Rizzuto, T. Pozzan, Microdomains of intracellular Ca^{2+}: molecular determinants and functional consequences, Physiol. Rev. 86 (2006) 369–408.
[32] S.C. Brazer, B.B. Singh, X. Liu, W. Swaim, I.S. Ambudkar, Caveolin-1 contributes to assembly of store-operated Ca^{2+} influx channels by regulating plasma membrane localization of TRPC1, J. Biol. Chem. 278 (2003) 27208–27215.
[33] T.P. Lockwich, X. Liu, B.B. Singh, J. Jadlowiec, S. Weiland, I.S. Ambudkar, Assembly of Trp1 in a signaling complex associated with caveolin-scaffolding lipid raft domains, J. Biol. Chem. 275 (2000) 11934–11942.
[34] R. Malli, M. Frieden, K. Osibow, C. Zoratti, M. Mayer, N. Demaurex, W.F. Graier, Sustained Ca^{2+} transfer across mitochondria is essential for mitochondrial Ca^{2+} buffering, sore-operated Ca^{2+} entry, and Ca^{2+} store refilling, J. Biol. Chem. 278 (2003) 44769–44779.
[35] M.G. Lee, X. Xu, W. Zeng, J. Diaz, R.J. Wojcikiewicz, T.H. Kuo, F. Wuytack, L. Racymaekers, S. Muallem, Polarized expression of Ca^{2+} channels in pancreatic and salivary gland cells. Correlation with initiation and propagation of $[Ca^{2+}]_i$ waves, J. Biol. Chem. 272 (1997) 15765–15770.
[36] H. Takemura, Y. Horio, Spatial microenvironment defines Ca^{2+} entry and Ca^{2+} release in salivary gland cells, Biochem. Biophys. Res. Commun. 336 (2005) 223–231.
[37] C. Hisatsune, K. Mikoshiba, Novel compartment implicated in calcium signaling—is it an “induced coupling domain”? Sci. STKE 2005 (2005) 53.
[38] A.A. Gerencser, V. Adam-Vizi, Mitochondrial Ca^{2+} dynamics reveals limited intramitochondrial Ca^{2+} diffusion, Biophys. J. 88 (2005) 698–714.